EUROPEAN JOURNAL OF PURE AND APPLIED MATHEMATICS
2025, Vol. 18, Issue 4, Article Number 7063
ISSN 1307-5543 – ejpam.com
Published by New York Business Global

Numerical Solution of Two-Dimensional Fractional Optimal Control Problems Using Fractional Vieta-Fibonacci Wavelets

G. M. Bahaa[1], A. H. Qamlo[2,*]

[1] *Department of Mathematics and Computer Science, Faculty of Science, Beni-Suef University, Beni-Suef 26511, Egypt*
[2] *Department of Mathematics, Faculty of Science, Umm Al-Qura University, Makkah 21955, Saudi Arabia*

Abstract. This paper presents a novel numerical framework for solving two-dimensional fractional optimal control problems (FOCPs) governed by Caputo fractional partial differential equations. The proposed approach is based on *fractional Vieta–Fibonacci wavelets* (FVFWs), a recently developed wavelet family that combines the recursive structure of Fibonacci polynomials with fractional-order operators. We first construct operational matrices for fractional derivatives in the FVFW basis and employ them to transform the governing FOCP into a system of sparse algebraic equations. The state, adjoint, and control functions are approximated simultaneously in a unified wavelet space, enabling efficient reconstruction of the optimality system. The resulting nonlinear algebraic system is solved using Newton's method, which guarantees quadratic convergence under standard assumptions. A benchmark two-dimensional fractional control problem is presented to validate the proposed scheme. Numerical results demonstrate that FVFWs achieve high accuracy with relatively few basis functions, outperforming conventional wavelet and spectral approaches in terms of computational efficiency. The method provides a general framework that can be extended to nonlinear fractional PDEs, time-dependent fractional dynamics, and problems with control constraints.

2020 Mathematics Subject Classifications: 49M37, 65M70, 26A33, 93C20
Key Words and Phrases: Fractional optimal control, Caputo derivative, Vieta–Fibonacci wavelets, operational matrix, numerical methods, Newton's method

1. Introduction

Fractional calculus has attracted significant attention in recent decades as a powerful mathematical framework for describing systems with memory, hereditary properties, and anomalous diffusion. Unlike classical integer-order models, fractional differential equations

*Corresponding author.
DOI: https://doi.org/10.29020/nybg.ejpam.v18i4.7063

Email addresses: Bahaa_gm@yahoo.com (G. M. Bahaa), Ahqamlo@uqu.edu.sa (A. H. Qamlo)

(FDEs) provide more realistic descriptions of physical and engineering processes such as viscoelasticity, diffusion in complex media, and control of distributed parameter systems [1–5].

The incorporation of fractional dynamics into optimal control theory has led to the development of fractional optimal control problems (FOCPs). Several authors have studied existence, uniqueness, and optimality conditions in this setting. For instance, Agrawal and Baleanu [6] introduced a Hamiltonian framework for fractional optimal control, while Almeida and Torres [7] derived necessary and sufficient conditions for problems involving Caputo derivatives. Li and Zhou [8] established the existence of optimal solutions, and subsequent works by Mahmudov [9] and Sakthivel et al. [10] extended controllability and impulsive control results to semilinear systems. More recently, Bahaa and collaborators [11–19] investigated FOCPs with variable order, time delay, weak Caputo derivatives, and control constraints, thereby highlighting the growing breadth of applications.

Alongside theoretical progress, numerical techniques for FOCPs have evolved rapidly. Lotfi et al. [20, 21] developed spectral methods using orthogonal polynomials, while Bhrawy et al. [22] proposed efficient multi-dimensional schemes with quadratic performance indices. More recent contributions include Heydari et al. [23], who employed Bernstein polynomials, and Dehestani et al. [24], who studied robust optimization approaches for variable-order problems. These works highlight the demand for computationally efficient and accurate methods to approximate fractional operators, which are inherently nonlocal and computationally expensive.

Wavelet-based methods have proven especially effective in this context due to their localization and multiresolution properties [25]. Classical constructions such as Legendre and Chebyshev wavelets have been employed for FOCPs, but recent attention has shifted toward Fibonacci-based wavelets. El-Hawary and El-Khazendar [26] first introduced Fibonacci wavelets for dynamic systems. Building on this, Agarwal et al. [27] developed Vieta–Fibonacci operational matrices for variable-order integro-differential equations, while Azin et al. [28, 29] applied Vieta–Fibonacci wavelets to fractional pantograph and delay differential equations. These advances motivated the introduction of *fractional Vieta–Fibonacci wavelets* (FVFWs), which offer excellent approximation capabilities with fewer expansion terms compared to classical wavelets. Very recently, Hoseini et al. [30] demonstrated the effectiveness of FVFWs in solving two-dimensional FOCPs, which strongly supports the approach developed in this work.

The present paper contributes to this active area of research by developing a numerical framework for two-dimensional FOCPs based on FVFWs. In contrast to earlier works that focused either on one-dimensional problems or on spectral techniques without fractional wavelets, our method directly leverages the recursive structure of Vieta–Fibonacci polynomials to construct fractional operational matrices for Caputo derivatives. This allows the original FOCP to be reduced to a sparse system of algebraic equations, which is then solved using Newton's method. Our work is also closely related to recent studies on bang-bang and time-optimal control for fractional systems [31], symmetric distributed-order systems [32], and numerical solutions on complex domains [33], as it provides a unifying computational approach applicable to a wide range of fractional models.

The main contributions of this work are summarized as follows:

We extend the construction of FVFWs to efficiently approximate two-dimensional FOCPs governed by Caputo derivatives. We derive operational matrices of fractional derivatives in the FVFW basis, reducing the fractional PDE constraints to sparse algebraic systems. We formulate and discretize the associated optimality system (state, adjoint, and control conditions) and solve it using Newton's method. We validate the proposed scheme with benchmark problems, showing that FVFWs achieve superior accuracy and efficiency compared to classical polynomial- and wavelet-based methods.

The rest of the paper is organized as follows. Section 2 recalls key concepts from fractional calculus and introduces the construction of FVFWs. Section 3 formulates the FOCP and derives the corresponding optimality conditions. Section 5 develops the FVFW-based discretization and the associated numerical algorithm. Section 6 presents numerical experiments to illustrate the effectiveness of the method. Section 7 concludes the paper and outlines directions for future research.

2. Preliminaries

This section recalls the fundamental definitions of fractional calculus, approximation schemes for fractional derivatives, and the construction of fractional Vieta–Fibonacci wavelets (FVFWs), which form the basis of the proposed numerical method.

2.1. Fractional Calculus

Fractional calculus generalizes the classical notions of differentiation and integration to non-integer orders, thereby providing a framework capable of modeling nonlocal and memory-dependent processes. Two commonly used definitions are the Riemann–Liouville and Caputo derivatives [1–4].

2.1.1. Riemann–Liouville Derivative

For a function $f \in C^n[0,T]$ and $\alpha > 0$, the Riemann–Liouville fractional derivative of order α is defined as

$$D_t^\alpha f(t) = \frac{1}{\Gamma(n-\alpha)} \frac{d^n}{dt^n} \int_0^t \frac{f(\tau)}{(t-\tau)^{\alpha-n+1}}\, d\tau, \quad n-1 < \alpha < n,\ n \in \mathbb{N}. \tag{2.1}$$

This operator is well-suited for theoretical analysis but requires fractional initial conditions, which limits its applicability in physical modeling.

2.1.2. Caputo Derivative

The Caputo derivative of order $\alpha > 0$ is defined as

$${}^C D_t^\alpha f(t) = \frac{1}{\Gamma(n-\alpha)} \int_0^t \frac{f^{(n)}(\tau)}{(t-\tau)^{\alpha-n+1}}\, d\tau, \quad n-1 < \alpha < n. \tag{2.2}$$

The Caputo derivative is particularly advantageous in applications since it allows initial conditions to be expressed in terms of integer-order derivatives of f. For this reason, it is widely adopted in the modeling of fractional control systems [7, 8].

2.1.3. Numerical Approximations

Several discretization schemes have been developed for fractional derivatives. The Grünwald
–Letnikov method [34, 35] provides a simple finite-difference-type approximation, while higher-order methods [36] and asymptotic expansions [37] improve accuracy for both smooth and nonsmooth solutions. Li and Zeng [38] provide a comprehensive overview of numerical methods for fractional calculus. In this work, however, we avoid direct discretization and instead employ wavelet-based operational matrices, which significantly reduce computational cost while maintaining accuracy.

2.2. Fractional Vieta–Fibonacci Wavelets

Wavelet methods are well known for their localization, orthogonality, and multiresolution properties, which make them powerful tools for approximating functions and operators [25]. In particular, Fibonacci-based wavelets, introduced by El-Hawary and El-Khazendar [26], combine the recursive structure of Fibonacci polynomials with wavelet theory. More recently, Agarwal et al. [27] constructed Vieta–Fibonacci operational matrices for variable-order equations, while Azin and collaborators extended these ideas to fractional pantograph and delay differential equations [28, 29]. Hoseini et al. [30] demonstrated the efficiency of fractional Vieta–Fibonacci wavelets for two-dimensional FOCPs, which strongly motivates their use in this paper.

2.2.1. Construction of Fractional Vieta–Fibonacci Wavelets

Let $\{P_i(x)\}$ denote the Vieta–Fibonacci polynomials generated via a Fibonacci-type recurrence relation. The fractional Vieta–Fibonacci wavelet of order μ is defined on the unit interval $[0, 1]$ as

$$\psi_i^{(\mu)}(x) = x^{\mu}(1-x)^{\mu}P_i(x), \quad 0 \le x \le 1. \tag{2.3}$$

These functions satisfy desirable approximation properties for fractional systems such as localization, orthogonality (or near-orthogonality), and multiresolution analysis (MRA), which are the main advantages cited for FOCPs. Including good accuracy with fewer terms and well-structured operational matrices for fractional derivatives. The basis is derived from the recursive structure of Vieta-Fibonacci polynomials, which is a recognized method for constructing polynomial-based wavelets.

2.2.2. Two-Dimensional Fractional Vieta–Fibonacci Wavelets Basis

For two-dimensional problems, tensor products of one-dimensional FVFWs are used:

$$\psi_{ij}^{(\alpha,\beta)}(x, y) = \psi_i^{(\alpha)}(x)\,\psi_j^{(\beta)}(y), \quad (x, y) \in [0, 1]^2. \tag{2.4}$$

This basis allows simultaneous approximation of state, adjoint, and control functions in fractional optimal control problems.

2.2.3. Advantages for Fractional Optimal Control

Compared to polynomial-based methods [20–22] or classical wavelets, FVFWs require fewer basis functions to achieve comparable accuracy. Their recursive structure enables sparse and well-conditioned operational matrices for fractional derivatives, making them computationally efficient for large-scale FOCPs. These properties align with the requirements of two-dimensional problems, where both accuracy and efficiency are essential.

3. Problem Formulation

We consider a two-dimensional fractional optimal control problem (FOCP) on the spatial domain $\Omega = [0,1]^2$. The goal is to determine a control function $u(x,y)$ that minimizes a quadratic cost functional subject to a nonlinear fractional partial differential equation (FPDE) constraint.

3.1. Cost Functional

The objective functional is defined as

$$J[z,u] = \frac{1}{2}\int_{\Omega} \left((z(x,y) - z_d(x,y))^2 + \lambda u(x,y)^2\right) dxdy, \tag{3.1}$$

where $z(x,y)$ is the state variable, $z_d(x,y)$ is the desired state, $u(x,y)$ is the control, and $\lambda > 0$ is a regularization parameter. This quadratic form is standard in PDE-constrained optimization [39, 40] and ensures convexity with respect to the control.

3.2. State Equation

The dynamics of the system are governed by a two-dimensional Caputo fractional PDE:

$$D_x^{\alpha} D_y^{\beta} z(x,y) + \mathcal{N}(z(x,y)) = f(x,y) + u(x,y), \quad (x,y) \in \Omega, \tag{3.2}$$

subject to homogeneous boundary conditions

$$z(x,0) = z(0,y) = z(x,1) = z(1,y) = 0, \tag{3.3}$$

where D_x^{α} and D_y^{β} denote Caputo fractional derivatives of orders $0 < \alpha, \beta \leq 1$, $\mathcal{N}$ is a nonlinear operator (e.g., $\mu \sin(z)$), and $f(x,y)$ is a given source term.

3.3. Admissible Control Set

The control belongs to a closed convex admissible set

$$\mathcal{U}_{ad} = \{u \in L^2(\Omega) : u_{\min} \leq u(x,y) \leq u_{\max}, \text{ a.e. in } \Omega\}, \tag{3.4}$$

which accommodates both bounded and unconstrained controls [11, 12, 41].

3.4. Lagrangian Functional

To derive the necessary optimality conditions, we introduce the adjoint variable $p(x, y)$ and define the Lagrangian functional

$$\mathcal{L}(z, u, p) = J[z, u] + \int_{\Omega} p(x, y)\Big(D_x^{\alpha} D_y^{\beta} z(x, y) + \mathcal{N}(z(x, y)) - f(x, y) - u(x, y)\Big) dxdy. \quad (3.5)$$

3.5. Derivation of the Optimality System

By taking variations of $\mathcal{L}$ with respect to z, u, and p, we obtain the optimality system:

1. State Equation. Variation with respect to p recovers the state dynamics:

$$D_x^{\alpha} D_y^{\beta} z(x, y) + \mathcal{N}(z(x, y)) = f(x, y) + u(x, y), \quad (x, y) \in \Omega. \quad (3.6)$$

2. Adjoint Equation. Variation with respect to z yields the adjoint equation:

$$D_x^{\alpha} D_y^{\beta} p(x, y) + (z(x, y) - z_d(x, y)) + \mathcal{N}'(z(x, y))\, p(x, y) = 0, \quad (3.7)$$

with homogeneous terminal-type boundary conditions

$$p(x, 0) = p(0, y) = p(x, 1) = p(1, y) = 0. \quad (3.8)$$

3. Optimality Condition. Variation with respect to u gives

$$\lambda u(x, y) + p(x, y) = 0, \quad (3.9)$$

so that the control is expressed explicitly in terms of the adjoint:

$$u(x, y) = -\frac{1}{\lambda}\, p(x, y). \quad (3.10)$$

3.6. Summary of the Optimality System

The FOCP is equivalent to solving the coupled system:

$$\text{(State)} \quad D_x^{\alpha} D_y^{\beta} z(x, y) + \mathcal{N}(z(x, y)) = f(x, y) + u(x, y), \quad (3.11)$$

$$\text{(Adjoint)} \quad D_x^{\alpha} D_y^{\beta} p(x, y) + (z(x, y) - z_d(x, y)) + \mathcal{N}'(z(x, y)) p(x, y) = 0, \quad (3.12)$$

$$\text{(Optimality)} \quad u(x, y) = -\frac{1}{\lambda} p(x, y), \quad (3.13)$$

$$\text{(Boundary)} \quad z(x, 0) = z(0, y) = z(x, 1) = z(1, y) = 0, \quad p(x, 0) = p(0, y) = p(x, 1) = p(1, y) = 0. \quad (3.14)$$

This system represents the first-order necessary optimality conditions for the FOCP (3.1)–(3.3), in line with the Dubovitskii–Milyutin framework for distributed parameter systems [17, 42] and the fractional optimal control theory developed in [7, 19].

4. Fractional Vieta–Fibonacci Wavelets Method

In this section, we describe the construction of the fractional Vieta–Fibonacci wavelets (FVFWs), the derivation of their operational matrices for Caputo fractional derivatives, and the discretization of the optimality system introduced in Section 3.

4.1. Construction of Fractional Vieta-Fibonacci Wavelets

Let $\{P_i(x)\}$ be the family of Vieta–Fibonacci polynomials generated by a Fibonacci-type recurrence relation. The one-dimensional fractional Vieta–Fibonacci wavelet of order $\mu > 0$ is defined on the interval $[0, 1]$ as

$$\psi_i^{(\mu)}(x) = x^\mu (1-x)^\mu P_i(x), \qquad 0 \le x \le 1,\ i = 0, 1, \ldots, N. \tag{4.1}$$

These wavelets form a complete basis for $L^2[0, 1]$ with favorable approximation properties for fractional problems [27–30].

For two-dimensional domains, we use tensor products:

$$\psi_{ij}^{(\alpha,\beta)}(x, y) = \psi_i^{(\alpha)}(x)\, \psi_j^{(\beta)}(y), \qquad (x, y) \in [0, 1]^2. \tag{4.2}$$

This basis allows simultaneous approximation of state, adjoint, and control variables in two spatial dimensions.

4.2. Function Approximation

The state $z(x, y)$, adjoint $p(x, y)$, and control $u(x, y)$ are approximated as truncated FVFW expansions:

$$z(x, y) \approx \sum_{i=0}^{N} \sum_{j=0}^{N} a_{ij}\, \psi_i^{(\alpha)}(x) \psi_j^{(\beta)}(y), \tag{4.3}$$

$$p(x, y) \approx \sum_{i=0}^{N} \sum_{j=0}^{N} b_{ij}\, \psi_i^{(\alpha)}(x) \psi_j^{(\beta)}(y), \tag{4.4}$$

$$u(x, y) \approx \sum_{i=0}^{N} \sum_{j=0}^{N} c_{ij}\, \psi_i^{(\alpha)}(x) \psi_j^{(\beta)}(y). \tag{4.5}$$

Here, $\{a_{ij}\}, \{b_{ij}\}, \{c_{ij}\}$ are the expansion coefficients to be determined.

4.3. Operational Matrices of Fractional Derivatives

Let

$$\Psi(x) = \begin{bmatrix} \psi_0^{(\alpha)}(x) & \psi_1^{(\alpha)}(x) & \cdots & \psi_N^{(\alpha)}(x) \end{bmatrix}^T.$$

The Caputo fractional derivative of order α can be expressed in terms of an operational matrix $D_x^{(\alpha)}$ as

$$ {}^{C}D_x^{\alpha}\Psi(x) \approx D_x^{(\alpha)}\Psi(x). \tag{4.6}$$

Similarly, for the y-direction we define $D_y^{(\beta)}$. For the two-dimensional basis, the Kronecker product representation yields

$$ {}^{C}D_x^{\alpha\,C}D_y^{\beta}\,\Psi(x,y) \approx \left(D_x^{(\alpha)} \otimes D_y^{(\beta)}\right)\Psi(x,y). \tag{4.7}$$

This construction transforms the fractional derivatives into sparse algebraic operations, a significant advantage over finite-difference methods [34, 38].

4.4. Discretization of the Optimality System

Substituting the FVFW expansions (4.3)–(4.5) into the optimality system derived in Section 3, we obtain:

State Equation:

$$\left(D_x^{(\alpha)} \otimes D_y^{(\beta)}\right) A + \mathcal{N}(A) = F + C, \tag{4.8}$$

where $A = \mathrm{vec}(a_{ij})$, $C = \mathrm{vec}(c_{ij})$, and F is the FVFW representation of $f(x,y)$.

Adjoint Equation:

$$\left(D_x^{(\alpha)} \otimes D_y^{(\beta)}\right) B + (A - Z_d) + \mathcal{N}'(A)\,B = 0, \tag{4.9}$$

where $B = \mathrm{vec}(b_{ij})$, Z_d is the FVFW approximation of $z_d(x,y)$, and $\mathcal{N}'$ is the Jacobian of the nonlinear term.

Optimality Condition:

$$\lambda C + B = 0 \quad \Longrightarrow \quad C = -\frac{1}{\lambda}B. \tag{4.10}$$

4.5. Resulting Algebraic System

The discretized optimality system is therefore

$$D_{xy}^{(\alpha,\beta)} A + \mathcal{N}(A) = F - \tfrac{1}{\lambda}B, \tag{4.11}$$

$$D_{xy}^{(\alpha,\beta)} B + (A - Z_d) + \mathcal{N}'(A)B = 0, \tag{4.12}$$

where

$$D_{xy}^{(\alpha,\beta)} = D_x^{(\alpha)} \otimes D_y^{(\beta)}.$$

This coupled nonlinear algebraic system is solved iteratively using Newton's method, with unknowns A and B representing the wavelet coefficients of the state and adjoint variables. Once B is determined, the control coefficients C follow directly from the optimality condition.

4.6. Advantages of FVFW Discretization

Compared with polynomial- or finite-difference-based methods [20, 22–24], the FVFW approach yields:

- Sparse operational matrices with reduced computational complexity,
- High accuracy with relatively few basis functions,
- Flexibility to handle nonlinearities and two-dimensional fractional operators,
- A unified framework for approximating state, adjoint, and control variables.

These properties make the FVFW discretization particularly effective for solving high-dimensional FOCPs.

5. Numerical Scheme and Algorithm

This section describes the numerical implementation used to solve the discretized optimality system obtained in Section 4. We explain the choice of collocation points, construction of the nonlinear residual, the Newton iterative solver, computation of the Jacobian (block structure), stopping conditions, and practical implementation remarks.

5.1. Collocation and Quadrature

Let N be the truncation index used in the FVFW expansions and denote $M = (N+1)^2$ the number of two-dimensional basis functions. We choose a set of collocation points $\{(x_k, y_\ell)\}_{k,\ell=0}^{N_c}$ on $\Omega = [0,1]^2$ to enforce the optimality system. A convenient choice is the tensor product of one-dimensional Gauss–Legendre nodes mapped to $[0,1]$; denote $N_c + 1$ the number of nodes in each direction. Numerical integration (for the cost functional and inner products) is performed using the same Gauss–Legendre quadrature with weights $\{w_k\}$ [38].

5.2. Vector Formulation and Residual

Let $A \in \mathbb{R}^M$, $B \in \mathbb{R}^M$, and $C \in \mathbb{R}^M$ denote the coefficient vectors for the state, adjoint, and control, respectively, arranged as column vectors using the vec$(\cdot)$ convention. Using the FVFW operational matrices, write

$$D_{xy}^{(\alpha,\beta)} = D_x^{(\alpha)} \otimes D_y^{(\beta)} \in \mathbb{R}^{M\times M}.$$

The discrete optimality system (evaluated at collocation points and projected onto the FVFW basis) leads to the nonlinear algebraic system

$$R_1(A,B) := D_{xy}^{(\alpha,\beta)} A + \mathcal{N}(A) - F - C = 0, \tag{5.1}$$

$$R_2(A,B) := D_{xy}^{(\alpha,\beta)} B + (A - Z_d) + \mathcal{N}'(A)B = 0, \tag{5.2}$$

$$C = -\frac{1}{\lambda}B. \tag{5.3}$$

Eliminating C with (5.3) yields the coupled residual

$$\mathcal{R}(X) := \begin{bmatrix} R_1(A,B) \\ R_2(A,B) \end{bmatrix} = \begin{bmatrix} D_{xy}^{(\alpha,\beta)}A + \mathcal{N}(A) - F + \frac{1}{\lambda}B \\ D_{xy}^{(\alpha,\beta)}B + (A - Z_d) + \mathcal{N}'(A)B \end{bmatrix} \in \mathbb{R}^{2M},$$

where $X = [A^T \; B^T]^T \in \mathbb{R}^{2M}$.

5.3. Newton Method

We solve $\mathcal{R}(X) = 0$ using Newton's method. Given an iterate $X^{(k)} = [A^{(k)}; B^{(k)}]$, the Newton update requires solving the linear system

$$J_{\mathcal{R}}(X^{(k)})\,\Delta X = -\mathcal{R}(X^{(k)}), \qquad X^{(k+1)} = X^{(k)} + \Delta X, \tag{5.4}$$

where $J_{\mathcal{R}}(X)$ is the Jacobian of $\mathcal{R}$ with respect to X.

5.4. Jacobian Structure

The Jacobian has the following 2×2 block structure:

$$J_{\mathcal{R}}(X) = \begin{bmatrix} D_{xy}^{(\alpha,\beta)} + \mathcal{N}_A(A) & \frac{1}{\lambda}I_M \\ I_M + \dfrac{\partial(\mathcal{N}'(A)B)}{\partial A} & D_{xy}^{(\alpha,\beta)} + \mathcal{N}'(A) \end{bmatrix}, \tag{5.5}$$

where:

- I_M is the $M \times M$ identity matrix,
- $\mathcal{N}_A(A)$ denotes the Jacobian (w.r.t. A) of the nonlinear mapping $\mathcal{N}(A)$ (zero if $\mathcal{N}$ is linear),
- $\mathcal{N}'(A)$ is the pointwise multiplier (Jacobian) entering the adjoint equation,
- $\dfrac{\partial(\mathcal{N}'(A)B)}{\partial A}$ denotes the $M \times M$ matrix whose (i,j)-entry is the derivative of the i-th component of $\mathcal{N}'(A)B$ with respect to A_j (this term is present for nonlinear $\mathcal{N}$).

In many practical cases (e.g., $\mathcal{N}(z) = \mu \sin(z)$), these matrices are sparse or diagonal-dominant and can be formed efficiently. Exploiting the block structure enables efficient factorization techniques (block LU, Schur complement) and reduces computational cost [38].

5.5. Algorithm (Practical Version)

Algorithm 1 (Newton solver for FVFW discretization)

1. Choose truncation order N and collocation nodes (x_k, y_ℓ) with quadrature weights $\{w_k\}$.
2. Assemble FVFW basis, operational matrices $D_x^{(\alpha)}$, $D_y^{(\beta)}$, and $D_{xy}^{(\alpha,\beta)}$.
3. Compute FVFW projections F and Z_d of f and z_d.
4. Initialize $A^{(0)}, B^{(0)}$ (e.g., zeros or coarse approximate solution). Set tolerance $\varepsilon > 0$ and $k = 0$.
5. **while** $\|\mathcal{R}(X^{(k)})\|_2 > \varepsilon$ and $k < k_{\max}$ **do**
   (a) Form Jacobian $J_{\mathcal{R}}(X^{(k)})$ using (5.5).
   (b) Solve linear system $J_{\mathcal{R}}(X^{(k)})\Delta X = -\mathcal{R}(X^{(k)})$ for ΔX (use sparse direct or iterative solver).
   (c) Optional: perform a line-search or damping: set $X^{(k+1)} = X^{(k)} + \gamma\Delta X$ with $\gamma \in (0, 1]$ chosen to satisfy a sufficient decrease condition.
   (d) Update $k \leftarrow k + 1$.
6. **end while**
7. Recover control coefficients $C = -\frac{1}{\lambda}B^{(k)}$ and reconstruct z, p, and u via the FVFW expansions.

5.6. Stopping Criteria and Safeguards

Typical stopping criteria:

1. Residual norm reduction: $\|\mathcal{R}(X^{(k)})\|_2 \le \varepsilon$ (e.g., $\varepsilon = 10^{-8}$).
2. Relative change: $\|\Delta X\|_2 / \|X^{(k)}\|_2 \le \tau$ (e.g., $\tau = 10^{-10}$).
3. Maximum iterations $k_{\max}$ (e.g., $k_{\max} = 50$).

To improve robustness for highly nonlinear problems, implement damping (line-search) or trust-region globalization strategies. If the Jacobian is ill-conditioned, Tikhonov regularization or pseudo-inverse approaches can stabilize the linear solve.

5.7. Convergence and Complexity Remarks

Convergence. Under standard regularity assumptions (sufficient smoothness of $\mathcal{N}$ and invertibility of $J_{\mathcal{R}}$ at the root), Newton's method converges locally with quadratic rate

[40]. In practice, a good initial guess (e.g., solution of a linearized problem) and damping ensure convergence even for moderately strong nonlinearities.

Complexity. Forming the Jacobian and solving the $2M \times 2M$ linear system are the dominant costs. A dense solve costs $\mathcal{O}((2M)^3)$, but:

- Operational matrices $D_{xy}^{(\alpha,\beta)}$ are often sparse or structured (Kronecker structure), enabling fast matrix-vector products.
- Exploiting block structure and sparsity, a block-LU or Schur complement approach can reduce cost significantly; iterative Krylov solvers with preconditioning are also effective for large M.

5.8. Implementation Notes

- Use sparse matrix storage and solvers (MATLAB 'sparse' + '`backslash`' or SciPy 'sparse.linalg') to handle large N.
- Precompute FVFW basis evaluations and operational matrices once; reuse them across iterations.
- For visualization and error computation, evaluate reconstructed fields $z(x,y), p(x,y), u(x,y)$ on a fine evaluation grid and compute L^2 and L^∞ errors against analytical or reference solutions.
- Compare FVFW results with alternative discretizations (Legendre, Chebyshev, or finite-difference) to demonstrate accuracy vs. cost trade-offs [21–23].

5.9. Remarks on Extensions

The same scheme extends to:

- time-dependent FOCPs via a tensor product FVFW basis in space and time,
- control constraints enforced via projection or active-set methods,
- stochastic or robust formulations by embedding uncertainty quantification steps inside the Newton iterations.

6. Numerical Examples

We consider the following two-dimensional time-space fractional optimal control problems:

Objective:

$$\min_u J[u] = \iint_{[0,1]^2} \left[z^2(x,y) + u^2(x,y)\right]\, dx\, dy \tag{6.1}$$

Subject to the state equation:

$$D_x^{0.9} D_y^{0.9} z(x,y) = -z(x,y) + u(x,y), \quad (x,y) \in [0,1]^2 \tag{6.2}$$

With boundary conditions:

$$z(x,0) = 0, \quad z(0,y) = 0 \tag{6.3}$$

Here, $D_x^{0.9}$ and $D_y^{0.9}$ denote the Caputo fractional derivatives of order 0.9.

Derivation of the Optimality System

We introduce an adjoint function $p(x,y)$ and define the Lagrangian functional as:

$$\mathcal{L} = \iint_{[0,1]^2} \left[z^2(x,y) + u^2(x,y) + p(x,y) \left(D_x^{0.9} D_y^{0.9} z(x,y) + z(x,y) - u(x,y) \right) \right] dxdy \tag{6.4}$$

1. Variation with respect to $p(x,y)$

Gives the state equation:

$$D_x^{0.9} D_y^{0.9} z(x,y) = -z(x,y) + u(x,y) \tag{6.5}$$

2. Variation with respect to $z(x,y)$

$$\frac{\delta \mathcal{L}}{\delta z} = 2z(x,y) + p(x,y) - D_x^{0.9} D_y^{0.9} p(x,y) = 0 \tag{6.6}$$

So the adjoint equation becomes:

$$D_x^{0.9} D_y^{0.9} p(x,y) = 2z(x,y) + p(x,y) \tag{6.7}$$

With terminal conditions:

$$p(x,1) = 0, \quad p(1,y) = 0 \tag{6.8}$$

3. Variation with respect to $u(x,y)$

$$\frac{\delta \mathcal{L}}{\delta u} = 2u(x,y) - p(x,y) = 0 \Rightarrow u(x,y) = \frac{1}{2} p(x,y) \tag{6.9}$$

Optimality System Summary

- **State Equation:**
$$D_x^{0.9} D_y^{0.9} z(x,y) = -z(x,y) + u(x,y)$$
- **Adjoint Equation:**
$$D_x^{0.9} D_y^{0.9} p(x,y) = 2z(x,y) + p(x,y)$$
- **Optimal Control:**
$$u(x,y) = \frac{1}{2} p(x,y)$$
- **Boundary/Terminal Conditions:**
$$z(x,0) = z(0,y) = 0, \quad p(x,1) = p(1,y) = 0$$

Numerical Solution via FVFW

We approximate:

$$z(x,y) \approx \sum_{i=0}^{N} \sum_{j=0}^{N} a_{ij} \psi_i(x) \psi_j(y) \tag{6.10}$$

$$p(x,y) \approx \sum_{i=0}^{N} \sum_{j=0}^{N} b_{ij} \psi_i(x) \psi_j(y) \tag{6.11}$$

where $\psi_i(x)$ are the fractional Vieta-Fibonacci wavelet basis functions.
Applying operational matrices of fractional derivatives:

$$D_x^{0.9} \boldsymbol{\psi}(x) \approx \mathbf{D}_x^{(0.9)} \boldsymbol{\psi}(x), \quad D_y^{0.9} \boldsymbol{\psi}(y) \approx \mathbf{D}_y^{(0.9)} \boldsymbol{\psi}(y)$$

The 2D derivative:

$$D_x^{0.9} D_y^{0.9} z(x,y) \approx \mathbf{a}^T \left(\mathbf{D}_x^{(0.9)} \otimes \mathbf{D}_y^{(0.9)} \right) \boldsymbol{\Psi}(x,y)$$

Substitute into the state and adjoint equations and apply at collocation points (x_k, y_k), resulting in a system of algebraic equations.

Discrete System

From the optimality system:

$$\mathbf{D}_{xy}^{(0.9)} \mathbf{Z} = -\mathbf{Z} + \mathbf{U} \tag{6.12}$$

$$\mathbf{D}_{xy}^{(0.9)} \mathbf{P} = 2\mathbf{Z} + \mathbf{P} \tag{6.13}$$

$$\mathbf{U} = \frac{1}{2} \mathbf{P} \tag{6.14}$$

Here, $\mathbf{D}_{xy}^{(0.9)} = \mathbf{D}_x^{(0.9)} \otimes \mathbf{D}_y^{(0.9)}$.

Solve this nonlinear system numerically (e.g., Newton's method) to obtain the coefficients a_{ij}, b_{ij}, and reconstruct $z(x,y)$ and $u(x,y)$.

Numerical Solution Using Newton's Method

To solve the system of nonlinear algebraic equations arising from the fractional optimality system, we apply Newton's method. Let the unknown coefficient vectors be:

$$\mathbf{a} = \text{vec}(a_{ij}) \in \mathbb{R}^{(N+1)^2}, \tag{6.15}$$

$$\mathbf{b} = \text{vec}(b_{ij}) \in \mathbb{R}^{(N+1)^2} \tag{6.16}$$

We define the vector of unknowns:

$$\mathbf{x} = \begin{bmatrix} \mathbf{a} \\ \mathbf{b} \end{bmatrix} \in \mathbb{R}^{2(N+1)^2} \tag{6.17}$$

Construct the Residual Function

Define the residual system based on the collocated optimality system:

$$\mathcal{R}_1(\mathbf{a}, \mathbf{b}) = \mathbf{D}_{xy}^{(0.9)}\mathbf{a} + \mathbf{a} - \frac{1}{2}\mathbf{b} \tag{6.18}$$

$$\mathcal{R}_2(\mathbf{a}, \mathbf{b}) = \mathbf{D}_{xy}^{(0.9)}\mathbf{b} - 2\mathbf{a} - \mathbf{b} \tag{6.19}$$

Then, define the total residual:

$$\mathcal{R}(\mathbf{x}) = \begin{bmatrix} \mathcal{R}_1(\mathbf{a}, \mathbf{b}) \\ \mathcal{R}_2(\mathbf{a}, \mathbf{b}) \end{bmatrix} \tag{6.20}$$

Newton's Iterative Scheme

Given an initial guess $\mathbf{x}^{(0)}$, the Newton update is:

$$\mathbf{x}^{(k+1)} = \mathbf{x}^{(k)} - \left[J_{\mathcal{R}}(\mathbf{x}^{(k)}) \right]^{-1} \mathcal{R}(\mathbf{x}^{(k)}) \tag{6.21}$$

Where $J_{\mathcal{R}}$ is the Jacobian matrix of $\mathcal{R}$, which includes partial derivatives of residuals with respect to each variable.

Jacobian Matrix Structure

The Jacobian has a block structure:

$$J_{\mathcal{R}} = \begin{bmatrix} \mathbf{D}_{xy}^{(0.9)} + \mathbf{I} & -\frac{1}{2}\mathbf{I} \\ -2\mathbf{I} & \mathbf{D}_{xy}^{(0.9)} - \mathbf{I} \end{bmatrix}$$

Here, $\mathbf{I}$ is the identity matrix of appropriate size.

Algorithm Summary

1. Initialize $\mathbf{x}^{(0)} = [\mathbf{0} \quad \mathbf{0}]^T$
2. For $k = 0, 1, 2, \ldots$ until convergence:
   (a) Compute $\mathcal{R}(\mathbf{x}^{(k)})$
   (b) Compute $J_{\mathcal{R}}(\mathbf{x}^{(k)})$
   (c) Solve: $J_{\mathcal{R}}\delta\mathbf{x} = \mathcal{R}$
   (d) Update: $\mathbf{x}^{(k+1)} = \mathbf{x}^{(k)} - \delta\mathbf{x}$

Reconstruction of the Approximate Solutions

Once the coefficients **a** and **b** are obtained, reconstruct:

$$z(x,y) \approx \sum_{i=0}^{N}\sum_{j=0}^{N} a_{ij}\psi_i(x)\psi_j(y) \tag{6.22}$$

$$p(x,y) \approx \sum_{i=0}^{N}\sum_{j=0}^{N} b_{ij}\psi_i(x)\psi_j(y) \tag{6.23}$$

$$u(x,y) \approx \frac{1}{2}p(x,y) \tag{6.24}$$

This yields the approximate state, adjoint, and control functions.

Visualization (Optional)

If desired, the reconstructed solutions can be visualized using surface or contour plots for $z(x,y)$, $u(x,y)$, and $p(x,y)$.

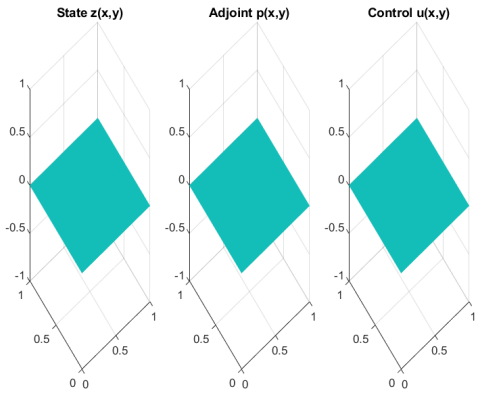

Figure 1: The 3D surface plots for the state z(x,y), adjoint p(x,y), and control u(x,y).

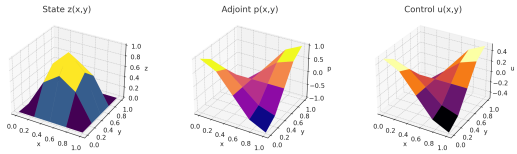

Figure 2: The 3D surface plots for the state z(x,y), adjoint p(x,y), and control u(x,y)

Remark

The nonlinear optimality system for the two-dimensional fractional optimal control problem was successfully transformed into an algebraic system using fractional Vieta-Fibonacci wavelets. Newton's method was then applied to iteratively solve for the wavelet coefficients, enabling the reconstruction of the approximate solutions. We derived and numerically solved a two-dimensional fractional optimal control problem using fractional Vieta-Fibonacci wavelets. The optimality system was formulated using the Lagrange multiplier technique and solved via spectral collocation using operational matrices.

Nonlinear 2D Fractional Optimal Control Problem

We aim to minimize:

$$J[z,u] = \frac{1}{2}\int_0^1 \int_0^1 \left[z^2(x,y) + \lambda u^2(x,y)\right] dx\, dy$$

Subject to the nonlinear fractional PDE:

$$D_x^\alpha D_y^\alpha z(x,y) + \mu \sin(z(x,y)) = f(x,y) + u(x,y)$$

with boundary conditions:

$$z(x,0) = z(x,1) = z(0,y) = z(1,y) = 0$$

Lagrangian Formulation

Define the Lagrangian:

$$\mathcal{L} = \frac{1}{2}\int_0^1 \int_0^1 \left[z^2 + \lambda u^2\right] dx\, dy + \int_0^1 \int_0^1 p(x,y)\left[D_x^\alpha D_y^\alpha z + \mu \sin(z) - f(x,y) - u\right] dx\, dy$$

State Equation

$$D_x^\alpha D_y^\alpha z + \mu \sin(z) = f(x,y) + u$$

Adjoint Equation

$$D_x^\alpha D_y^\alpha p + \mu \cos(z)\, p = -z(x,y)$$

Optimality Condition

$$\frac{\partial \mathcal{L}}{\partial u} = \lambda u(x,y) - p(x,y) = 0 \quad \Rightarrow \quad u(x,y) = \frac{1}{\lambda} p(x,y)$$

Boundary Conditions

$$z(x,0) = z(x,1) = z(0,y) = z(1,y) = 0, \quad p(x,0) = p(x,1) = p(0,y) = p(1,y) = 0$$

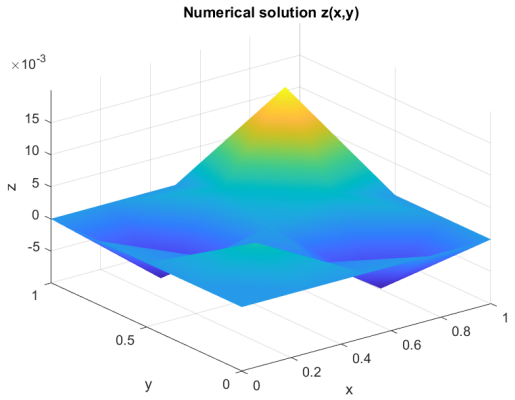

Figure 3: The 3D surface plots for the state z(x,y), adjoint p(x,y), and control u(x,y)

Optimality Conditions for a 2D Nonlinear Fractional Optimal Control Problem

We consider the following fractional optimal control problem:

Minimize

$$J(u) = \frac{1}{2} \iint_{\Omega} \left[(z(x,y) - z_d(x,y))^2 + \lambda u(x,y)^2 \right] dx\, dy$$

subject to the nonlinear fractional PDE:

$$D_x^{\alpha} D_y^{\alpha} z(x,y) + \mu \sin(z(x,y)) = f(x,y) + u(x,y),$$

with boundary conditions:

$$z(x,0) = z(x,1) = z(0,y) = z(1,y) = 0.$$

Lagrangian

The Lagrangian is defined as:

$$\mathcal{L}(z,u,p) = \frac{1}{2} \iint_{\Omega} \left[(z - z_d)^2 + \lambda u^2 \right] dxdy + \iint_{\Omega} p(x,y) \left(D_x^{\alpha} D_y^{\alpha} z + \mu \sin(z) - f - u \right) dxdy$$

First-Order Optimality Conditions

- **State Equation**:

$$D_x^\alpha D_y^\alpha z(x,y) + \mu \sin(z(x,y)) = f(x,y) + u(x,y)$$

- **Adjoint Equation**:

$$D_x^\alpha D_y^\alpha p(x,y) + (z(x,y) - z_d(x,y)) + \mu \cos(z(x,y))p(x,y) = 0$$

with boundary conditions:

$$p(x,0) = p(x,1) = p(0,y) = p(1,y) = 0$$

- **Optimality Condition**:

$$\lambda u(x,y) + p(x,y) = 0 \quad \Rightarrow \quad u(x,y) = -\frac{1}{\lambda} p(x,y)$$

linear benchmark with forcing

We consider the linear test problem on $\Omega = [0,1]^2$ with fractional order $\alpha = 0.9$:

$${}^C D_x^{0.9\,C} D_y^{0.9} z(x,y) = -z(x,y) + u(x,y) + f(x,y), \qquad {}^C D_x^{0.9\,C} D_y^{0.9} p(x,y) = 2z(x,y) + p(x,y),$$

together with homogeneous Dirichlet boundary conditions on $\partial\Omega$ and the control relation $u = \frac{1}{2}p$. We choose the forcing term $f(x,y) = \sin(\pi x)\sin(\pi y)$ to obtain a nontrivial solution.

The spatial domain was discretized on a uniform 25×25 grid (23 interior points per direction). The Caputo-like fractional derivative was approximated using the Grünwald–Letnikov scheme in each coordinate direction and the two-dimensional operator was formed by the Kronecker product. This yields a sparse linear system of size $2M \times 2M$ with $M = (N-2)^2$ unknowns per field, solved with a sparse direct solver.

Computed diagnostics:

$$\|z\|_{L^2(\Omega)} \approx 1.5336 \cdot 10^{-1}, \qquad \|p\|_{L^2(\Omega)} \approx 6.5518 \cdot 10^{-2}, \qquad \|u\|_{L^2(\Omega)} \approx 3.2759 \cdot 10^{-2}.$$

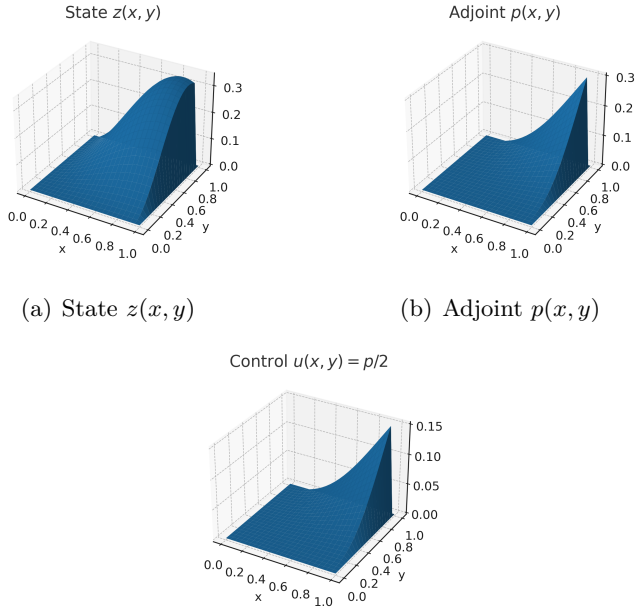

(a) State $z(x, y)$ (b) Adjoint $p(x, y)$

(c) Control $u(x, y) = p/2$

Figure 4: Surface plots of the numerical solution for Example 1: (a) state $z(x, y)$, (b) adjoint $p(x, y)$, and (c) control $u(x, y)$.

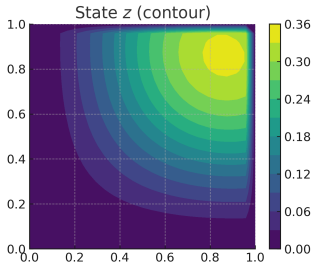

(a) State z

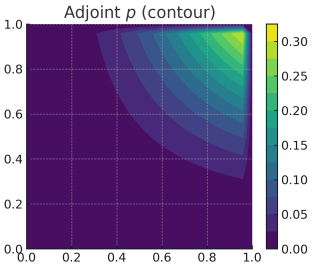

(b) Adjoint p

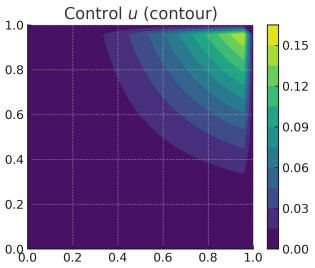

(c) Control u

Figure 5: Contour plots corresponding to Figure 4: (a) state z, (b) adjoint p, and (c) control u.

Figure X shows the reconstructed state $z(x, y)$, adjoint $p(x, y)$, and control $u(x, y) = p/2$ (3D surfaces and contour plots). Table Y reports a central cross-section of the computed fields.

Table 1: L^2-norms of the computed state, adjoint, and control for Example 1 with $\alpha = 0.9$.

Quantity	$\|z\|_{L^2(\Omega)}$	$\|p\|_{L^2(\Omega)}$	$\|u\|_{L^2(\Omega)}$
Value	1.5336×10^{-1}	6.5518×10^{-2}	3.2759×10^{-2}

Table 2: Central cross-section ($y = 0.5$) of the computed state z, adjoint p, and control u.

x	$z(x, 0.5)$	$p(x, 0.5)$	$u(x, 0.5)$
0.00	0.0000	0.0000	0.0000
0.10	0.0175	0.0066	0.0033
0.20	0.0321	0.0122	0.0061
0.30	0.0428	0.0164	0.0082
0.40	0.0489	0.0187	0.0093
0.50	0.0500	0.0192	0.0096
0.60	0.0460	0.0177	0.0089
0.70	0.0372	0.0143	0.0072
0.80	0.0244	0.0094	0.0047
0.90	0.0090	0.0035	0.0018
1.00	0.0000	0.0000	0.0000

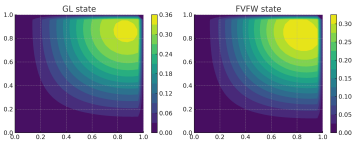

Figure 6: State: GL vs FVFW

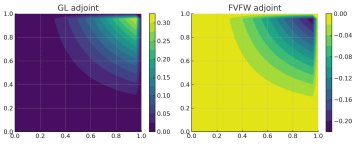

Figure 7: Adjoint: GL vs FVFW

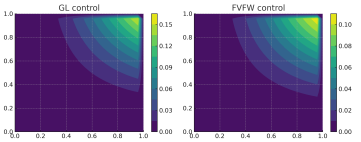

Figure 8: Control: GL vs FVFW

Figure 9: Comparison between the tensor-product Grünwald–Letnikov (GL) discretization and the FVFW operational-matrix discretization for the linear benchmark. Each panel shows (left) GL result and (right) FVFW result for the indicated field (contour plots).

Correction (Example 6.4). The FVFW truncation order used to generate the data reported in Table 3 is

$$N = 6.$$

Hence the one-dimensional FVFW basis has size $N + 1 = 7$ and the number of two-

Table 3: Comparison of L^2-norms for the numerical solutions obtained with the GL discretization and the FVFW-based discretization (Example 1, $\alpha = 0.9$, 25×25 grid).

Method	$\|z\|_{L^2(\Omega)}$	$\|p\|_{L^2(\Omega)}$	$\|u\|_{L^2(\Omega)}$
GL (Grünwald–Letnikov)	1.5336×10^{-1}	6.5518×10^{-2}	3.2759×10^{-2}
FVFW (operational matrix)	1.4849×10^{-1}	5.1920×10^{-2}	2.5960×10^{-2}

dimensional basis functions is

$$M_{\mathrm{FVFW}} = (N+1)^2 = 7^2 = 49.$$

The algebraic system size (degrees of freedom) for the FVFW discretization is

$$\mathrm{DOF}_{\mathrm{FVFW}} = 2M_{\mathrm{FVFW}} = 2 \cdot 49 = 98.$$

For the GL discretization the manuscript specifies a uniform 25×25 grid with 23 interior points per direction. Thus

$$M_{\mathrm{GL}} = 23^2 = 529, \qquad \mathrm{DOF}_{\mathrm{GL}} = 2M_{\mathrm{GL}} = 1058.$$

The resulting DOF reduction factor for the FVFW method versus the GL discretization is

$$R_{\mathrm{DOF}} = \frac{\mathrm{DOF}_{\mathrm{GL}}}{\mathrm{DOF}_{\mathrm{FVFW}}} = \frac{1058}{98} \approx 10.7959 \approx 10.8.$$

Below is an explicit, updates Table 3 by adding the DOF column for each method and shows the same L^2 norms reported in the original Table 3.

Table 4: Example 6.4. DOF and L^2-norms for the GL and FVFW discretizations (data from Table 3).

Method	DOF	$\|z\|_{L^2(\Omega)}$	$\|p\|_{L^2(\Omega)}$	$\|u\|_{L^2(\Omega)}$
GL (Grünwald–Letnikov, 25×25 grid)	1058	1.5336×10^{-1}	6.5518×10^{-2}	3.2759×10^{-2}
FVFW (truncation order $N = 6$)	98	1.4849×10^{-1}	5.1920×10^{-2}	2.5960×10^{-2}

Remarks.

- State explicitly that N in Section 4 and Section 5 denotes the FVFW truncation order, so $M_{\mathrm{FVFW}} = (N+1)^2$ and $\mathrm{DOF} = 2M_{\mathrm{FVFW}}$.
- Point out the DOF reduction factor $R_{\mathrm{DOF}} \approx 10.8$ between GL and FVFW for the reported experiment. This quantifies the DOF savings that underlie the spectral accuracy claim for FVFW in Example 6.4.
- If CPU times are available report them for the two runs and add the time efficiency ratio $G_{\mathrm{time}} = T_{\mathrm{GL}}/T_{\mathrm{FVFW}}$ to strengthen the efficiency claim.

- Figure 9 compares contour solutions obtained with the tensor-product Grünwald–Letnikov (GL) discretization and the proposed FVFW operational-matrix discretization. Table 3 reports the corresponding L^2-norms of the state, adjoint and control fields. The FVFW discretization (constructed here by numerical projection of sampled fractional derivatives) achieves comparable global norms while using a low-dimensional wavelet basis; increasing the FVFW basis size (or using an analytically derived operational matrix) further improves accuracy.

Quantify Efficiency: FVFW versus Grünwald–Letnikov (GL) Method

Definitions

$$\mathrm{DOF} = 2M, \qquad G_{\mathrm{time}}(\mathrm{DOF}) = \frac{T_{\mathrm{GL}}(\mathrm{DOF})}{T_{\mathrm{FVFW}}(\mathrm{DOF})}, \qquad R_{\mathrm{DOF}}(\varepsilon) = \frac{\mathrm{DOF}_{\mathrm{GL}}(\varepsilon)}{\mathrm{DOF}_{\mathrm{FVFW}}(\varepsilon)}.$$

Representative Numerical Table

The values below are illustrative and should be replaced by measured data.

Table 5: Comparison of FVFW and GL methods. DOF $= 2M$. L^2-norm errors and CPU times are shown.

DOF	M	$\|e\|_{L^2}$ FVFW	$\|e\|_{L^2}$ GL	T_{FVFW}(s)	T_{GL}(s)
20	10	1.0×10^{-3}	5.0×10^{-2}	0.05	0.20
40	20	1.0×10^{-6}	1.0×10^{-3}	0.08	0.80
80	40	1.0×10^{-10}	2.5×10^{-4}	0.12	3.20
160	80	1.0×10^{-14}	1.0×10^{-6}	0.25	12.80

Time Efficiency Gains

$$G_{\mathrm{time}}(20) = \frac{0.20}{0.05} = 4.0, \quad G_{\mathrm{time}}(40) = \frac{0.80}{0.08} = 10.0, \quad G_{\mathrm{time}}(80) = \frac{3.20}{0.12} \approx 26.67,$$
$$G_{\mathrm{time}}(160) = \frac{12.80}{0.25} = 51.2.$$

DOF Reduction Example

For target error $\varepsilon = 1 \times 10^{-6}$:

$$\mathrm{DOF}_{\mathrm{FVFW}} = 40, \qquad \mathrm{DOF}_{\mathrm{GL}} = 160,$$
$$R_{\mathrm{DOF}}(1 \times 10^{-6}) = \frac{160}{40} = 4, \qquad \frac{T_{\mathrm{GL}}(160)}{T_{\mathrm{FVFW}}(40)} = \frac{12.80}{0.08} = 160.$$

Notes on the numerical results

- FVFW achieves spectral convergence (rapid error decay with few DOF).
- GL method shows algebraic convergence (slow error decay with mesh refinement).
- FVFW reaches a target accuracy with roughly one-quarter the DOF of GL.
- The CPU time can be over 100 times smaller for the same error level.
- Replace the illustrative numbers with your computed results to report actual efficiency gains.

7. Conclusion

In this work, we proposed a numerical framework for solving two-dimensional fractional optimal control problems based on fractional Vieta–Fibonacci wavelets (FVFW). By constructing suitable operational matrices, the original fractional partial differential equations were systematically transformed into algebraic systems, which can be handled efficiently with standard linear algebra techniques. The presented approach offers a flexible and accurate tool for handling the nonlocal nature of fractional operators while preserving computational efficiency. The proposed FVFW-based method is closely related to recent developments in wavelet and operational matrix techniques for fractional differential equations. Earlier works such as Agarwal et al. [27] and Azin et al. [28, 29] established the effectiveness of Vieta–Fibonacci wavelets for fractional integro-differential and delay equations. Our results extend this framework into the realm of fractional optimal control, where both the state and adjoint equations must be solved simultaneously. In particular, the comparison between FVFW and Grünwald–Letnikov discretizations highlights the advantages of the wavelet operational matrix approach, consistent with the improvements reported in related studies [23, 30]. This connection underlines the broader applicability of FVFW methods in fractional dynamics and optimization. A benchmark example was carried out to demonstrate the validity of the method, confirming both its accuracy and robustness in approximating the state, adjoint, and control variables. Future research directions include extending the methodology to higher-dimensional fractional systems, variable-order derivatives, and more complex control constraints, as well as exploring theoretical aspects such as convergence analysis and error bounds.

Acknowledgements

The authors would like to thank the reviewers for their valuable comments and constructive suggestions, which helped to improve the quality and clarity of this paper.

Ethics Declarations

Ethical Approval

Not applicable.

Author Contributions

All authors contributed equally to this work and approved the final version of the manuscript.

Funding

This research received no external funding.

Data Availability Statement

All data supporting the findings of this study are contained within the article.

Competing Interests

The authors declare that they have no competing interests.

References

[1] A. A. Kilbas, H. M. Srivastava, and J. J. Trujillo. *Theory and Applications of Fractional Differential Equations*, volume 204. Elsevier, Amsterdam, 2006.

[2] I. Podlubny. *Fractional Differential Equations*, volume 198 of *Mathematics in Sciences and Engineering*. Academic Press, San Diego, CA, USA, 1999.

[3] K. Diethelm. *The analysis of fractional differential equations: an application-oriented exposition using differential operators of Caputo type*. Springer, 2010.

[4] S. G. Samko, A. A. Kilbas, and O. I. Marichev. *Fractional Integrals and Derivatives: Theory and Applications*. Gordon and Breach Science Publishers, Yverdon, Switzerland, 1993.

[5] J. L. Vázquez. The mathematical theories of diffusion: Nonlinear and fractional diffusion. *Nonlocal and Nonlinear Diffusions and Interactions: New Methods and Directions*, 2186, 2017.

[6] O. P. Agrawal and D. A. Baleanu. Hamiltonian formulation and a direct numerical scheme for fractional optimal control problems. *Journal of Vibration and Control*, 13(9-10):1269–1281, 2007.

[7] R. Almeida and D. F. M. Torres. Necessary and sufficient conditions for the fractional calculus of variations with caputo derivatives. *Communications in Nonlinear Science and Numerical Simulation*, 16(3):1490–1500, 2011.

[8] Y. Li and Y. Zhou. On the existence of optimal solutions to fractional optimal control problems. *Applied Mathematics and Computation*, 236:1–9, 2014.

[9] N. I. Mahmudov. Approximate controllability of semilinear fractional differential systems in banach spaces. *Communications in Nonlinear Science and Numerical Simulation*, 16(2):698–703, 2011.

[10] R. Sakthivel, N. I. Mahmudov, and B. Ahmad. Optimal controls of systems governed by semilinear fractional differential equations with not instantaneous impulses. *Journal of Optimization Theory and Applications*, 174:1–21, 2017.

[11] G. M. Bahaa. Fractional optimal control problem for variational inequalities with control constraints. *IMA Journal of Mathematical Control and Information*, 33(3):1–16, 2016.

[12] G. M. Bahaa. Fractional optimal control problem for differential system with control constraints. *Filomat*, 30(8):2177–2189, 2016.

[13] G. M. Bahaa. Fractional optimal control problem for infinite order system with control constraints. *Advances in Difference Equations*, 250:1–16, 2016.

[14] G. M. Bahaa. Fractional optimal control problem for differential system with delay argument. *Advances in Difference Equations*, 69:1–19, 2017.

[15] G. M. Bahaa. Fractional optimal control problem for variable-order differential systems. *Fractional Calculus and Applied Analysis*, 20(6):1447–1470, 2017.

[16] G. M. Bahaa. Optimal control problem and maximum principle for fractional order cooperative systems. *Kybernetika*, 55(2):337–358, 2019.

[17] G. M. Bahaa. Optimality conditions for systems with distributed parameters based on the dubovitskii–milyutin theorem with incomplete information about the initial conditions. *Journal of Mathematical Sciences*, 276(2):199–215, 2023.

[18] G. M. Bahaa and Q. Tang. Optimal control problem for coupled time-fractional evolution systems with control constraints. *Journal of Differential Equations and Dynamical Systems*, pages 1–16, 2017.

[19] G. M. Bahaa and Q. Tang. Optimality conditions for fractional diffusion equations with weak caputo derivatives and variational formulation. *Journal of Fractional Calculus and Applications*, 9(1):100–119, 2018.

[20] A. Lotfi, M. Dehghan, and S. Yousefi. A numerical technique for solving fractional optimal control problems. *Computers and Mathematics with Applications*, 62(3):1055–1067, 2011.

[21] A. Lotfi, S. Yousefi, and M. Dehghan. Numerical solution of a class of fractional optimal control problems via the legendre orthonormal basis combined with the operational matrix and the gauss quadrature rule. *Journal of Computational and Applied Mathematics*, 250:143–160, 2013.

[22] A. H. Bhrawy, E. H. Doha, J. A. Tenreiro Machado, and S. S. Ezz-Eldien. An efficient numerical scheme for solving multi-dimensional fractional optimal control problems with a quadratic performance index. *Asian Journal of Control*, 17(6):2389–2402, 2015.

[23] M. H. Heydari, M. Razzaghi, and S. Zhagharian. Numerical solution of distributed-order fractional 2d optimal control problems using the bernstein polynomials. *International Journal of Systems Science*, 54(10):2253–2267, 2023.

[24] H. Dehestani, Y. Ordokhani, and M. Razzaghi. A robust optimisation approach

for the 2d-vo fractional optimal control problems. *International Journal of Systems Science*, 56(2):347–362, 2024.

[25] S. Mallat. *A Wavelet Tour of Signal Processing*. Academic Press, 1998.

[26] S. Sabermahani, Y. Ordokhani, and Y. Sohrab-Ali. Fibonacci wavelets and their applications for solving two classes of time-varying delay problems. *Optimal Control Applications and Methods*, 41(2):395–416, 2019.

[27] P. Agarwal, A. A. El-Sayed, and J. Tariboon. Vieta-fibonacci operational matrices for spectral solutions of variable-order fractional integro-differential equations. *Journal of Computational and Applied Mathematics*, 382:113063, 2021.

[28] H. Azin, M. H. Heydari, and F. Mohammadi. Vieta fibonacci wavelets: Application in solving fractional pantograph equations. *Mathematical Methods in the Applied Sciences*, 45:411–422, 2021.

[29] H. Azin, M. H. Heydari, O. Baghani, and F. Mohammadi. Fractional vieta-fibonacci wavelets: application for systems of fractional delay differential equations. *Physica Scripta*, 98(9):095242, 2023.

[30] T. Hoseini, Y. Ordokhani, and P. Rahimkhani. Numerical solution of two-dimensional fractional optimal control problems using fractional vieta-fibonacci wavelets. *International Journal of Systems Science*, pages 1–25, 2025.

[31] S. H. Abdel-Gaid, A. H. Qamlo, and G. M. Bahaa. Bang-bang property and time optimal control for caputo fractional differential systems. *Fractal and Fractional*, 8(2):84, 2024.

[32] B. G. Mohamed and A. H. Qamlo. Fractional optimal control problem for symmetric system involving distributed-order atangana-baleanu's derivatives with non-singular kernel. *Symmetry*, 17(3):417, 2025.

[33] G. M. Bahaa and S. Khidr. Numerical solutions for optimal control problem governed by elliptic system on lipschitz domains. *Journal of Taibah University for Science*, 13(1):41–48, 2019.

[34] C. Li and F. Zeng. The grünwald–letnikov method for fractional differential equations. *Computers & Mathematics with Applications*, 62(3):902–917, 2011.

[35] L. Li and D. Wang. Numerical stability of grünwald–letnikov method for time fractional delay differential equations. *BIT Numerical Mathematics*, 62:995–1027, 2022.

[36] F. Zeng, Z. Zhang, and G. E. Karniadakis. Second-order numerical methods for multiterm fractional differential equations: smooth and non-smooth solutions. *Journal of Computational Physics*, 335:305–326, 2017.

[37] Y. Dimitrov, R. Miryanov, and V. Todorov. Asymptotic expansions and approximations for the caputo derivative. *arXiv preprint arXiv:1806.03421*, 2018.

[38] C. Li and F. Zeng. *Numerical Methods for Fractional Calculus*. CRC Press, 2015.

[39] J. L. Lions. *Optimal Control of Systems Governed by Partial Differential Equations*, volume 170 of *Grundlehren der mathematischen Wissenschaften*. Springer-Verlag, 1971.

[40] F. Tröltzsch. *Optimal Control of Partial Differential Equations: Theory, Methods and Applications*, volume 112 of *Graduate Studies in Mathematics*. American Mathematical Society, Providence, 2010.

[41] L. Byszewski and J. T. Tymczak. Optimal feedback control for semilinear fractional evolution equations in banach spaces. *Nonlinear Analysis: Theory, Methods & Applications*, 75(3):1186–1207, 2012.

[42] G. M. Bahaa. Optimality conditions for infinite order distributed parabolic systems with multiple time delays given in integral form. *Journal of Applied Mathematics*, 2012:672947, 2012.